ISSN 0005-1179 (print), ISSN 1608-3032 (online), Automation and Remote Control, 2025, Vol. 86, No. 3, pp. 249–265.

CONTROL IN TECHNICAL SYSTEMS

Discrete-Time Controller Design for Multivariable Systems via Engineering Performance Indices

V. N. Chestnov[*,a] **and D. V. Shatov**[*,b]

[*] *Trapeznikov Institute of Control Sciences, Russian Academy of Sciences, Moscow, Russia*
e-mail: [a] *vnchest@yandex.ru,* [b] *dvshatov@gmail.com*

Received March 20, 2024
Revised December 6, 2024
Accepted December 17, 2024

Abstract—This paper is devoted to linear multivariable controlled plants subjected to unknown bounded external disturbances. We propose a method for designing discrete-time output-feedback controllers ensuring desired or achievable performance indices: accuracy, settling time, and stability margins for each control loop at the plant's input. The controller design approach is based on the standard H_∞ optimization procedure formulated in a particular way. Robust properties of the systems designed are investigated using the Nyquist plots of separate open control loops with break points at the plant's inputs. The absolute stability of the closed-loop system with sectoral nonlinearities at the plant's inputs and a relation with the radius of stability margins are proved. A numerical example is provided to demonstrate the effectiveness of this approach.

Keywords: linear multivariable systems, discrete-time controller design, bounded external disturbances, control errors, the radius of stability margins, settling time, absolute stability

DOI: 10.31857/S0005117925030051

1. INTRODUCTION

Digital controllers have taken a dominant position in manufacturing, power engineering, aviation, robotics, and many other industries. Therefore, following the real demands of design engineers, the problem of designing discrete-time controllers for multivariable systems via engineering performance indices becomes unprecedentedly topical and important.

At the same time, modern controller design methods based on a measured output—H_2, H_∞, and L_1 (l_1) optimization, μ-synthesis, and modal control—usually consider only some performance indices or even neglect them.

In classical automatic control theory, which involves frequency-domain methods with the Nyquist criterion, engineering performance indices were directly used to construct controllers for single-variable systems [1, 2]. These results were generalized largely due to the efforts of V.V. Solodovnikov in the well-known method of logarithmic amplitude response (Bode plot) [3, 4]. Note that the method has demonstrated unsurpassed practical effectiveness during the last 75 years. In the discrete-time case, it has acquired a complete form thanks to V.A. Besekerskii et al. [5, 6]. However, the inconsistency of engineering performance indices (accuracy, settling time, and stability margins) was evident even for single-variable systems. Unfortunately, due to its very essence, the method of logarithmic amplitude response is generally inapplicable to the class of multivariable systems. Difficulties in the mathematical formalization of engineering performance indices and the development of an appropriate apparatus fell out of mathematicians' sight for a long time. Only with the emergence of L_1 (l_1) optimization [7, 8] and H_∞ optimization [9–11], accuracy criteria (the maximum error for each controlled variable) under arbitrary bounded external disturbances

and the H_∞ norm of the sensitivity matrix have come to be used as accuracy and robustness indices in multivariate systems theory. At the same time, according to the analysis of the simplest examples [12], l_1 controllers give the maximum possible gain of an open-loop system if the closed-loop one is stable. However, this condition leads to small phase and gain margins determined using the Nyquist plot of the open-loop system, which is unacceptable in practice. In addition, discrete-time l_1 controllers may have an unpredictably high order [8], which is also not welcome in practice and inevitably decreases stability margins [12]. Continuous-time L_1 controllers are described by irrational transfer functions [7], which strongly reduces their potential in applications.

The method of invariant ellipsoids [13] has removed the fundamental limitations on the realizability of L_1 (l_1) controllers. Nevertheless, the issue of phase and gain margins acceptable from a practical point of view is still open in this promising approach.

In this paper, we estimate the stability margins of a system by their radius [14, 15]. By definition, this value is the maximum radius of the circle centered at the critical point $(-1,\ j0)$ that is not intersected by the Nyquist plot of an open-loop system; for example, see [16], where it was called "stability radius."

The design procedure of discrete-time controllers based on the measured output is complicated by the following important factors:

1. Generally speaking, even the full state-feedback controller [12, 17] does not ensure an acceptable radius of stability margins in practice. This is always possible only for stable plants under a small sampling period.

2. For discrete-time controllers based on the full state vector (the more so for those based on the output), the achievable control error is bounded below by some value that cannot be improved by any linear controller [18].

3. Even in the continuous-time case, the system's performance (characterized by the degree of stability) is limited by the absolute value of the real part of the plant's zero nearest to the imaginary axis [16, 19, 20]. In addition, increasing the degree of stability catastrophically reduces the radius of stability margins, which is not applicable in practice. Similar phenomena occur in the discrete-time case [12, 17].

This paper is devoted to the problem of designing discrete-time controllers for multivariable plants via given or achievable engineering performance indices: the control error for each controlled variable, the settling time, and the radius of stability margins at the plant's input. The solution involves an H_∞ optimization problem constructed in a special way. In this sense, the approach below develops the result of the earlier paper [17] by introducing unmeasured polyharmonic external disturbances with unknown amplitudes (with a bounded sum of harmonic amplitudes for each component of the disturbance), frequencies, and an unbounded number of them. Such a class of external disturbances covers all the real signals that cause controlled variables to deviate from zero in practical stabilization systems [21]. This paper is an extended version of the results presented in [22, 23].

2. PROBLEM STATEMENT

Consider a controllable and observable discrete-time model of a continuous-time plant described by the difference equations

$$\begin{gathered} x(k+1) = Ax(k) + B[u(k) + w(k)], \\ y(k) = Cx(k), \quad k = 0, 1, 2, \ldots, \end{gathered} \tag{1}$$

where $x(k) \in \mathbb{R}^n$ is the state vector of the plant, $u(k) \in \mathbb{R}^m$ is the control input of the plant, $y(k) \in \mathbb{R}^{m_2}$ is the measured and, simultaneously, controlled output of the plant (the controller's input), and $w(k) \in \mathbb{R}^m$ is the vector of external disturbances. The plant's matrices A, B, and C are known.

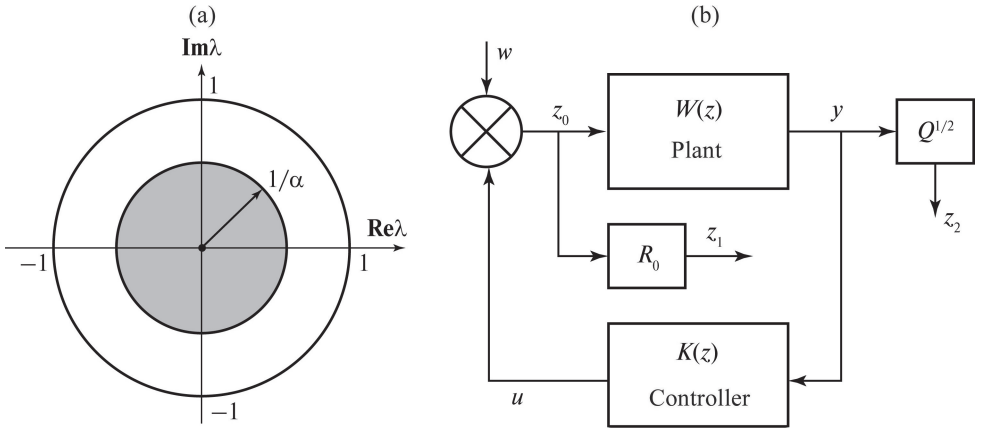

Fig. 1. (a) The arrangement of the eigenvalues of the matrix A_{cl} and (b) the block diagram of the closed-loop control system.

The plant (1) is closed by a discrete-time stabilizing dynamic output-feedback controller of the form

$$\begin{aligned} x_c(k+1) &= A_c x_c(k) + B_c y(k), \\ u(k) &= C_c x_c(k) + D_c y(k), \quad k = 0, 1, 2, \dots, \end{aligned} \tag{2}$$

where $x_c(k) \in \mathbb{R}^{n_c}$ is the state vector of the controller ($n_c \leqslant n$) and A_c, B_c, C_c, and D_c are numerical matrices.

The components of the external disturbance w are bounded functions:

$$w_i(k) = \sum_{j=1}^{\infty} w_{ij} \sin(\omega_j k h + \phi_{ij}), \quad i = \overline{1, m}, \tag{3}$$

where h is a sampling period. The amplitudes $w_{ij} \geqslant 0$, phases ϕ_{ij}, $i = \overline{1, m}$, and frequencies ω_j, $j = \overline{1, \infty}$, of the disturbance components are unknown.

By assumption, the external disturbance is bounded in the following sense:

$$\sum_{j=1}^{\infty} w_{ij} \leqslant w_i^*, \quad i = \overline{1, m}, \tag{4}$$

where w_i^* are given numbers. In other words, $\forall k \ |w_i(k)| \leqslant w_i^*$.

The errors for the controlled variables are defined by

$$y_{i,st} = \sup_{k \geqslant k_p} |y_i(k)|, \quad i = \overline{1, m_2}, \tag{5}$$

where the number k_p determines the settling time of the system, $t_p = k_p h$.

The number of cycles k_p is determined by the degree of stability of the discrete-time system, $1/\alpha$. This means the condition

$$|\lambda_i(A_{cl})| \leqslant \frac{1}{\alpha}, \quad i = \overline{1, n + n_c},$$

where $\lambda_i(\cdot)$ are the eigenvalues of the matrix A_{cl} of the closed-loop system (1), (2):

$$A_{cl} = \begin{bmatrix} A + BD_cC & BC_c \\ B_cC & A_c \end{bmatrix}.$$

Figure 1a provides the geometric interpretation of the last inequality for $\lambda_i(A_{cl})$.

In applications, the required value of α is assigned based on the desired number k_p ($t_p = k_p h$) as follows [17]:

$$\alpha \approx e^{(3h)/t_p}. \tag{6}$$

This condition is immediate from the well-known relation $\alpha = e^{\beta h}$ between the eigenvalues of continuous- and discrete-time systems. (That is, the degree of stability of a continuous-time system, β, and the settling time satisfy the approximate formula $t_p \approx 3/\beta$.) The relation (6) gives an acceptable estimation accuracy from the engineering point of view, provided that the eigenvalues of the matrix A_{cl} contain no multiples lying nearest to the circle of radius $1/\alpha$. As a rule, this requirement holds in applications.

The closed-loop system (1), (2) has the radii of stability margins $0 < r_i < 1$, $i = \overline{1,m}$, at the plant's physical input if the diagonal radii matrix $R = \operatorname{diag}[r_1, \ldots, r_m]$ satisfies the frequency-domain inequality [22]

$$\left[I + W(e^{-j\omega h})\right]^{\top} \left[I + W(e^{j\omega h})\right] > R^2, \quad \omega \in [0,\ \pi/h], \tag{7}$$

where $W(\mathrm{z}) = -K(\mathrm{z})W_0(\mathrm{z})$ is the transfer matrix of system (1), (2) with break points at the plant's physical input, $W_0(\mathrm{z}) = C(\mathrm{z}\,I - A)^{-1}B$ is the plant's transfer matrix relative to the control, and $K(\mathrm{z}) = C_c(\mathrm{z}\,I - A_c)^{-1}B_c + D_c$ is the transfer matrix of the controller.

The accuracy requirements for the system are specified by the inequalities

$$y_{i,st} \leqslant y_i^*, \quad i = \overline{1, m_2}, \tag{8}$$

where $y_i^* > 0$ are given numbers (the desired control errors).

Inequalities (8) are not always realizable: an appropriate controller cannot be found for some y_i^*, $i = \overline{1, m_2}$. The same concerns the requirements (6) and (7) for the settling time and the radii of stability margins. All these requirements are mutually contradictory [12].

Problem 1. It is required to find a stabilizing controller of the form (2) such that:

1) The accuracy requirements

$$y_{i,st} \leqslant \gamma y_i^*, \quad i = \overline{1, m_2}, \tag{9}$$

hold with some achievable number $\gamma > 0$.

2) System (1), (2) possesses some achievable radii of stability margins r_i, $i = \overline{1,m}$, in inequality (7).

3) The eigenvalues of the matrix A_{cl} of the closed-loop system (1), (2) satisfy the condition $|\lambda_i(A_{cl})| \leqslant 1/\alpha$, $i = \overline{1, n + n_c}$, where $\alpha > 1$ is some achievable number.

The coefficient γ in conditions (9) is some number, usually $\gamma > 1$. It indicates the degree to which the original accuracy requirements (8) are overestimated compared to the really achievable ones (9).

3. PROBLEM SOLUTION BASED ON H_∞ OPTIMIZATION

To solve Problem 1 using H_∞ optimization, we need to represent the closed-loop system equations (1), (2) in terms of transfer matrices:

$$\begin{gathered} y = W_0(\mathrm{z})z_0, \quad u = K(\mathrm{z})y, \\ z_0 = u + w, \quad z_1 = R_0 z_0, \quad z_2 = Q^{1/2} y, \end{gathered} \tag{10}$$

where $z_1 \in \mathbb{R}^m$ and $z_2 \in \mathbb{R}^{m_2}$ are the vectors of controlled variables used in the design procedure, with z_1 defining the desired radii of stability margins at the plant's input and z_2 ensuring accuracy; $R_0 = \operatorname{diag}[r_1^0, \ldots, r_m^0]$, $r_i^0 \in (0,1)$, $i = \overline{1,m}$, is the matrix of the desired radii of stability margins; finally, $Q^{1/2}$ is a diagonal weight matrix. Figure 1b shows the block diagram of the system of equations (10).

The vectors w and z_0 are related by the transfer matrix of sensitivity relative to the input,

$$T_{z_0 w} = [I + W(\mathrm{z})]^{-1}.$$

This matrix is used in the design procedure to ensure stability margins (7).

The vector of controlled variables $z_2 = Q^{1/2} y$ is introduced to satisfy the accuracy requirements (8), (9). It represents the vector y weighted by a diagonal matrix $Q = \operatorname{diag}[q_1, \ldots, q_{m_2}]$ with positive elements $q_i > 0$, $i = \overline{1, m_2}$. Appropriately assigned elements of the matrix Q ensure the required (or achievable) accuracy for the controlled variables y_i, $i = \overline{1, m_2}$; see the proof of this fact below.

Let us introduce the extended vector of controlled variables $z^\top = [z_1^\top,\ z_2^\top]$ and denote by T_{zw} the matrix relating z to the vector w. Then

$$z = \begin{bmatrix} z_1 \\ z_2 \end{bmatrix} = T_{zw} w = \begin{bmatrix} T_{z_1 w} \\ T_{z_2 w} \end{bmatrix} w = \begin{bmatrix} R_0 T_{z_0 w} \\ Q^{1/2} T_{yw} \end{bmatrix} w,$$

where $T_{yw} = W_0(\mathrm{z})[I + W(\mathrm{z})]^{-1}$ is the transfer matrix relating w and y.

The desired settling time is ensured if the eigenvalues of the matrix A_{cl} of the closed-loop system (1), (2) satisfy the inequality $|\lambda_i(A_{cl})| \leqslant 1/\alpha$. To ensure this condition, we apply the following technique [24]: replace the plant's matrices A and B with the shifted ones $\tilde{A} = \alpha A$ and $\tilde{B} = \alpha B$, respectively, and then find the shifted controller stabilizing the shifted closed-loop system:

$$\begin{gathered} |\lambda_i(\tilde{A}_{cl})| = |\lambda_i(A_{cl})|\alpha < 1, \quad i = \overline{1, n + n_c}, \\ \tilde{A}_{cl} = \begin{bmatrix} \tilde{A} + \tilde{B} D_c C & \tilde{B} C_c \\ \tilde{B}_c C & \tilde{A}_c \end{bmatrix}, \end{gathered} \tag{11}$$

where $\tilde{A}_c$, $\tilde{B}_c$, C_c, and D_c are the shifted controller's matrices.

For the original (unshifted) problem, the output-feedback controller (2) ensuring the desired degree of system stability (as well as the stability margin and accuracy requirements) has the following matrices [17, 24]:

$$A_c = \tilde{A}_c/\alpha, \quad B_c = \tilde{B}_c/\alpha, \quad C_c, \quad D_c. \tag{12}$$

Remark 1. An analog of the technique [24], albeit for full state-feedback controllers, is well known in the Western literature; for example, see [25]. For controllers based on the measured output in the continuous- and discrete-time cases, this approach was first proposed in Russia. In this context, we refer to [24] and the bibliography therein.

Let the controller with matrices $\tilde{A}_c$, $\tilde{B}_c$, C_c, and D_c minimize the H_∞ norm of the transfer matrix of the shifted closed-loop system (with matrices $\tilde{A}$ and $\tilde{B}$):

$$\|T_{zw}(e^{(-\beta + j\omega)h})\|_\infty < \gamma, \tag{13}$$

where γ is a given number or the value to be minimized.

Remark 2. If the shifted problem (13) is solved, the controller (2) with the matrices (12) will also ensure the corresponding frequency inequalities for the unshifted transfer matrix [17, 24]. Therefore, the solution of the shifted problem (13) satisfies the inequality

$$\|T_{zw}(e^{j\omega h})\|_\infty < \gamma \tag{14}$$

and, for each block of this matrix, we obtain the following condition similar to (14) (in particular, see [26]):

$$\|R_0 T_{z_0 w}(e^{j\omega h})\|_\infty < \gamma, \quad \|Q^{1/2} T_{yw}(e^{j\omega h})\|_\infty < \gamma. \tag{15}$$

The first inequality in (15) can be equivalently written as [17, 19]

$$[I + W(e^{-j\omega h})]^\top [I + W(e^{j\omega h})] > R^2, \quad \omega \in [0,\ \pi/h],$$

where $R = R_0/\gamma$ (see [27]). It represents the target inequality (7).

The second inequality in (15) has the equivalent form

$$T_{yw}^\top(e^{-j\omega h}) Q T_{yw}(e^{j\omega h}) < \gamma^2 I, \quad \omega \in [0,\ \pi/h]. \tag{16}$$

Lemma 1. *Under inequality* (16), *the errors for the controlled variables of the stable closed-loop system* (1), (2) *with disturbances from the class* (3), (4) *satisfy the inequalities*

$$q_i y_{i,st}^2 < \gamma^2 \left(\sum_j^m w_j^* \right)^2, \quad i = \overline{1, m_2}. \tag{17}$$

The proof of Lemma 1 is given in the Appendix.

With the elements of the diagonal weight matrix Q assigned by

$$q_i = \frac{\left(\sum_j^m w_j^*\right)^2}{(y_i^*)^2}, \quad i = \overline{1, m_2}, \tag{18}$$

inequalities (17) directly imply the target inequalities (9) of the problem under consideration.

Summarizing, we now formulate the main result of this paper.

Theorem 1. *The controller* (2) *with the matrices* (12) *solves Problem 1 if the coefficients of the weight matrix Q in the shifted H_∞ optimization problem* (13) *are assigned by* (18). *The radii of stability margins at the plant's input determine the diagonal matrix $R = R_0/\gamma$, where γ is obtained by solving problem* (13).

Here, the number γ (usually $\gamma \geqslant 1$) also determines the degree of achievability for the radii of stability margins given by the diagonal matrix R_0.

Note that passing from inequalities (13) to (14) and (15) makes the above results sufficient as well.

4. A PHYSICAL INTERPRETATION OF THE RADII OF STABILITY MARGINS

From the practical point of view, an important result can be obtained by studying the frequency matrix inequality (7) when breaking the control loop at only one ith input. This approach to analyzing the stability margins of systems matches engineering practice: it can be experimentally verified on a real plant. Let us introduce the following notation: $\mathrm{w}_i(\mathrm{z})$ is the transfer function of the system with break points at the ith input; $t_i(\mathrm{z})$ is the transfer function relating the ith component

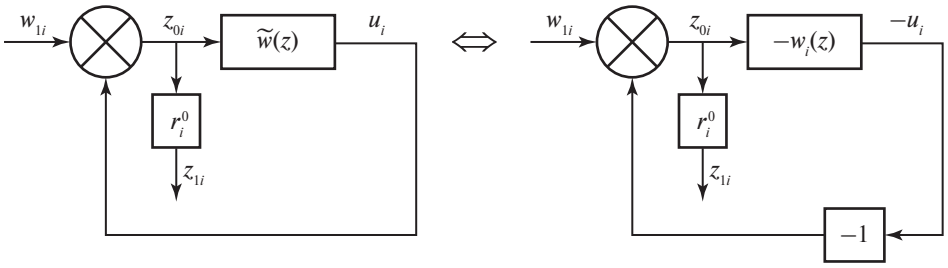

Fig. 2. The block diagram with the transfer function $\mathrm{w}_i(\mathrm{z})$.

of the vector w to the ith component of the vector z_1 (when all other inputs in Fig. 1b are zero). This break can be represented by the block diagram in the left-hand part of Fig. 2, where $\tilde{\mathrm{w}}(\mathrm{z})$ is the transfer function obtained by closing all feedback loops in Fig. 1b except for the ith one.

The right-hand part of Fig. 2 illustrates an equivalent form involving $\mathrm{w}_i(\mathrm{z})$; in this case, obviously, $\mathrm{w}_i(\mathrm{z}) = -\tilde{\mathrm{w}}(\mathrm{z})$.

The transfer functions $t_i(\mathrm{z})$ and $\mathrm{w}_i(\mathrm{z})$ are related to each other by the formula

$$t_i(\mathrm{z}) = r_i^0[1 + \mathrm{w}_i(\mathrm{z})]^{-1}. \tag{19}$$

On the other hand, the transfer function (19) is the ith diagonal element of the transfer matrix $T_{z_1 w}$. This matrix satisfies the first inequality in (15); for its ith diagonal element we have [26]

$$|t_i(e^{-j\omega h})| < \gamma \Leftrightarrow t_i(e^{-j\omega h})t_i(e^{j\omega h}) < \gamma^2.$$

Due to (19), this finally yields a scalar analog of (7):

$$[1 + \mathrm{w}_i(e^{-j\omega h})][1 + \mathrm{w}_i(e^{j\omega h})] > r_i^2, \quad i = \overline{1,m}, \quad \omega \in [0,\ \pi/h],$$

where $r_i = r_i^0/\gamma$.

This condition with its geometric interpretation [17, 26] leads to the following result.

Theorem 2. *Under the frequency matrix inequality* (7), *the Nyquist plot of system* (1), (2) *broken at the plant's ith input does not touch the circle of radius r_i centered at the critical point* $(-1,\ j0)$.

The radius r_i of stability margins can be determined via a real experiment, which is crucial in applications. If the open-loop system in Fig. 2 is stable, the Nyquist plot for $\mathrm{w}_i(e^{j\omega h})$ can be directly drawn. In the otherwise unstable case, it is necessary to take the frequency response of the closed-loop system shown in Fig. 2, which is the transfer function $t(e^{j\omega h})$ relating the ith components of the vectors w_1 and z_0 : $t(\mathrm{z}) = [1 + \mathrm{w}_i(\mathrm{z})]^{-1}$. Then the radius of stability margins equals $r_i = 1/\|t\|_\infty$, see [11, 15–17]. In other words, it is determined by the inverse of the maximum of the absolute value of the frequency response of the sensitivity function $t(e^{j\omega h})$ of the loop shown in Fig. 2.

According to Theorem 2, the Nyquist plot $\mathrm{w}(e^{j\omega h})$ does not intersect the closed interval $[-1 - r_i,\ -1 + r_i]$ of the real axis. In turn, by the circle criterion of absolute stability [28], system (1), (2) remains stable in this case if a nonstationary sector nonlinearity from the sector $\left[\frac{1}{1+r_i},\ \frac{1}{1-r_i}\right]$ is introduced into the ith input channel of the plant. For example, it can be a nonstationary gain $l_i(k)$ with an arbitrarily changing value within this interval.

The multivariable circle criterion allows strengthening this result for the case of nonlinearities introduced in each input channel. The closed-loop equations are written as

$$u = -W(\mathrm{z})\zeta, \quad \zeta = u. \tag{20}$$

Considering the design method of the controller (2), such a system is asymptotically stable, so the minimal stability condition of the circle criterion holds. The second (linear) equation in (20) is replaced by a vector nonlinearity of the form

$$\zeta = \phi[k,\ u(k)], \tag{21}$$

where each component of the nonstationary vector function $\zeta \in \mathbb{R}^m$ lies in a sector:

$$\alpha_i \leqslant \frac{\phi_i[k,\ u_i(k)]}{u_i(k)} \leqslant \beta_i, \quad \phi_i[k,\ 0] = 0, \quad i = \overline{1,m}, \tag{22}$$

where $\alpha_i < 1$ and $\beta_i > 1$ the lower and upper bounds of the sector nonlinearity.

According to the circle criterion [29, 30], system (20)–(22) is absolutely stable under the frequency inequality

$$\operatorname{Re}\left\{[I + \alpha W(e^{-j\omega h})]^\top \tau [I + \beta W(e^{j\omega h})]\right\} > 0, \quad \omega \in [-\pi/h,\ \pi/h], \tag{23}$$

where $\operatorname{Re}\{Y\} = [Y^\top(e^{-j\omega h}) + Y(e^{j\omega h})]/2$ denotes the Hermite part of the complex matrix Y. The matrix τ is a positive definite diagonal matrix, $\alpha = \operatorname{diag}\{\alpha_i\}$ and $\beta = \operatorname{diag}\{\beta_i\}$, $i = \overline{1,m}$, are diagonal matrices.

Condition (23) with the matrices $\alpha = \operatorname{diag}\left\{\frac{1}{1+r_i}\right\}$, $\beta = \operatorname{diag}\left\{\frac{1}{1-r_i}\right\}$ and $\tau = \operatorname{diag}\{(1+r_i)(1-r_i)\}$, $i = \overline{1,m}$ bring to the inequality

$$\operatorname{Re}\left\{[I + R + W(e^{-j\omega h})]^\top [I - R + W(e^{j\omega h})]\right\} > 0, \quad \omega \in [-\pi/h,\ \pi/h],$$

where $R = \operatorname{diag}\{r_i\}$ is a diagonal matrix. In turn, the last inequality implies

$$\operatorname{Re}\left\{[I + W(e^{-j\omega h})]^\top [I + W(e^{j\omega h})] - R^2 + V(e^{j\omega h})\right\} > 0, \quad \omega \in [-\pi/h,\ \pi/h],$$

where the skew Hermitian matrix $V(e^{j\omega h}) = RW(e^{j\omega h}) - W^\top(e^{j\omega h})R$ satisfies the condition $\operatorname{Re}\{V(e^{j\omega h})\} = 0$. This inequality can be represented in the form (7), and the following result is true accordingly.

Theorem 3. *Assume that Problem 1 is solved and/or the matrix inequality* (7) *holds. Then the nonlinear system* (1), (2), (12) *with nonstationary sector nonlinearities* (21) *from the class* (22) *with* $\alpha_i = 1/(1+r_i)$ *and* $\beta_i = 1/(1-r_i)$, $i = \overline{1,m}$, *introduced for each physical input channel of the plant* (1), *is absolutely stable* (*for* $w = 0$).

In a particular case, the nonlinearities can be treated as time-varying gains $l_i(k) : \zeta_i(k) = l_i(k)u_i(k)$ with the bounds α_i and β_i, $i = \overline{1,m}$ from Theorem 3, which can independently and arbitrarily change their values within the intervals specified. This fact emphasizes the robust properties of the systems designed.

5. A NUMERICAL EXAMPLE

As an illustrative example, we design a controller for the discretized model of a multi-motor electric drive of a pipe-electric welding machine, which was used in continuous time in [21, 31]. Such systems have clear applications and are known in the literature as parallel systems; see the Parallel Systems section in [32, Ch. 11].

Figure 3 shows the block diagram of this machine. The control actions u_1 and u_2 represent the voltages applied to the thyristor converters, which are modeled by inertial links with parameters $k_{\text{thyr}i}$ and $T_{\text{thyr}i}$, $i = 1, 2$, respectively. Their outputs x_i, $i = 1, 2$, are the output voltages of the

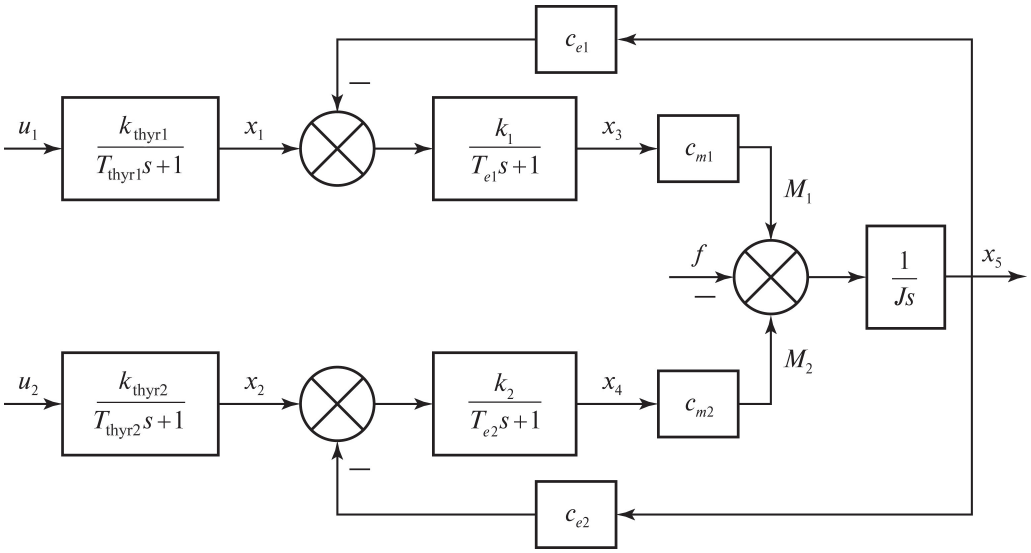

Fig. 3. The block diagram of the pipe-electric welding machine.

thyristor converters supplied to the armature circuits of the motors, which are modeled in the standard way using the parameters T_{ei} and k_i, $i = 1, 2$ (the electromagnetic time constants of the armature circuits and the corresponding gains); c_{mi} and c_{ei}, $i = 1, 2$, are the design constants of the motors. The states x_3 and x_4 represent the armature currents of the drive motors. The moments developed by the motors are denoted by $M_i = c_{mi}x_{i+2}$, $i = 1, 2$; finally, $f = M_{\text{loa}}$ is the total load resistance moment and J is the total moment of inertia reduced to one of the motor shafts. The state $x_5 = \omega$ is the angular velocity of the motor shafts (the main controlled variable). The measured variables are the currents of the motors and the angular velocity of their shafts. According to numerical experiments with the angular velocity of motors $y_3 = x_5$ taken as the only controlled variable, the equal-load requirement may fail for motors and, most importantly, the stability margins for the measured variables $y_1 = x_3$ and $y_2 = x_4$ (motor currents) at the plant's output may be very small [33], which is unacceptable in practice. Therefore, $y_1 = x_3$, $y_2 = x_4$, and $y_3 = x_5$ are chosen as the controlled variables. The numerical parameters of the model were described in [33].

Note an important feature of this model: the control actions u_1 and u_2 and the external disturbance are applied at essentially different points of the block diagram in Fig. 3. As a result, the design approach described above cannot be used directly. In addition, the internal feedback loops formed by the coefficients c_{ei}, $i = 1, 2$, reduce the effect of the disturbance f on the main controlled variable $x_5 = \omega$ (the angular velocity of the motor shafts). Let these loops be neglected, which worsens the plant in terms of accuracy. Then, having separated from $f = f_1 + f_2$ the resistance moments f_1 and f_2, applied to the first and second motors, respectively (as actually happens in practice) and assuming $f_1 = f_2$, we bring the disturbances to the plant's inputs u_1 and u_2 in the form of disturbances w_1 and w_2. In this case, the bounds f_1^* and f_2^* of the disturbances are recalculated into the bounds w_1^* and w_2^* by the formulas

$$w_i^* = \frac{f_i^*}{k_i c_{mi} k_{\text{thyr}i}}, \quad i = 1, 2,$$

which is true for constants f_1 and f_2. We will demonstrate that the worst-case disturbance for the closed-loop system with the controller designed by the above approach is indeed little different from the step disturbance in terms of the control error.

The continuous-time model of this machine is described by the state-space equations

$$\dot{x} = Ax + B_2 u + B_1 f, \quad y = Cx$$

with the numerical matrices

$$A = \begin{bmatrix} -100 & 0 & 0 & 0 & 0 \\ 0 & -83.33 & 0 & 0 & 0 \\ 137.81 & 0 & -11.29 & 0 & -1123.16 \\ 0 & 132.46 & 0 & -11.07 & -1101.13 \\ 0 & 0 & 0.25 & 0.25 & 0 \end{bmatrix},$$

$$B_1 = \begin{bmatrix} 0 \\ 0 \\ 0 \\ 0 \\ -0.03 \end{bmatrix}, \quad B_2 = \begin{bmatrix} 16\,120 & 0 \\ 0 & 13\,702 \\ 0 & 0 \\ 0 & 0 \\ 0 & 0 \end{bmatrix}, \quad C = \begin{bmatrix} 0 & 0 & 1 & 0 & 0 \\ 0 & 0 & 0 & 1 & 0 \\ 0 & 0 & 0 & 0 & 1 \end{bmatrix}.$$

The system is discretized with a period of $h = 0.01$ s.

According to Problem 1, the following requirements are imposed on the performance indices of the closed-loop system:

- Under $|f| \leqslant f^* = 600$ Nm, the desired errors for the controlled variables are

$$y_1^* = y_2^* = 375 \text{ A}, \quad y_3^* = 1 \text{ rad/s}.$$

  In addition, the system motors must be equally loaded: $y_{1,st} \approx y_{2,st}$.
- Achievable radii of stability margins for the control actions u_1 and u_2 must be ensured in the system.
- The desired settling time of the system is $t_p = 0.25$ s, which gives $\alpha = e^{(3h)/t_p} = 1.0618$ and, consequently, $|\lambda_i(A_{cl})| < 1/\alpha = 0.9418$.

The controller was designed in MATLAB by forming and solving the H_∞ optimization problem (13). To assign the diagonal weight matrix $Q^{1/2}$, we find the bounds of the equivalent external disturbances w_i, $i = 1, 2$, applied in accordance with the control actions. Using the above formulas for w_i^*, $i = 1, 2$, we obtain

$$w_1^* = \frac{f_1^*}{k_1 c_{m1} k_{\text{thyr1}}} = 0.0188 \text{ V}, \quad w_2^* = \frac{f_2^*}{k_2 c_{m2} k_{\text{thyr2}}} = 0.0185 \text{ V},$$

where $f_1^* = f_2^* = 300$ Nm, and the drive parameters correspond to [33]: $k_1 = 12.21$ 1/Ω, $c_{m1} = 8.1$ Nm/A, $k_{\text{thyr1}} = 161.2$, $k_2 = 11.965$ 1/Ω, $c_{m2} = 8.262$ Nm/A, and $k_{\text{thyr2}} = 164.424$. Finally, using (18), we obtain the weights

$$q_1^{1/2} = \frac{w_1^* + w_2^*}{y_1^*} \approx 10^{-4}\Omega, \; q_2^{1/2} = q_1^{1/2} \approx 10^{-4}\Omega, \; q_3^{1/2} = \frac{w_1^* + w_2^*}{y_3^*} = 0.037 \, \frac{\text{Vs}}{\text{rad}}.$$

The matrix R_0 of the desired radii of stability margins is assigned in the form

$$R_0 = \text{diag}[r^0 \quad r^0], \quad r^0 = 0.7.$$

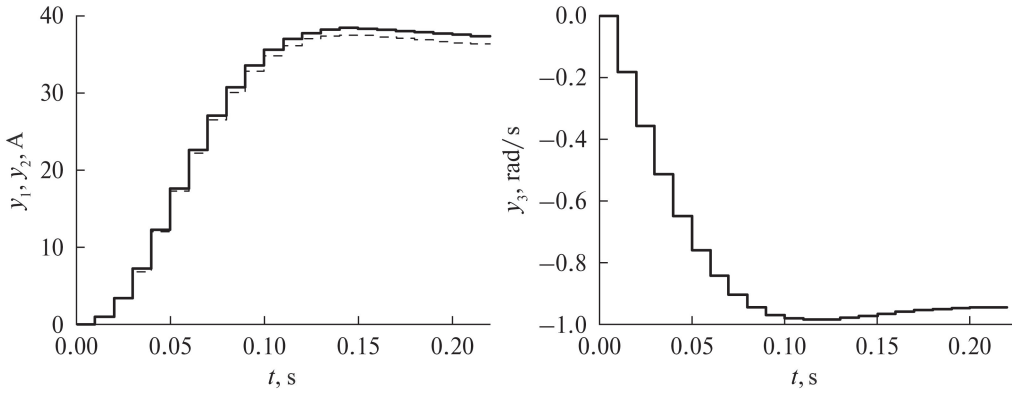

Fig. 4. Simulation of the closed-loop system under $f = 600$ Nm: the outputs y_1 and y_2 (left) and y_3 (right).

Solving the H_∞ optimization problem yielded the discrete-time controller $K(\mathrm{z})$ with the state-space matrices

$$A_c = \begin{bmatrix} 0.345956 & -0.009928 & -0.000697 & 0.0025 & -0.056187 \\ -0.008343 & -0.767521 & -0.017857 & -0.047834 & 0.007471 \\ 0.073728 & -0.017642 & -0.698692 & -6.373 \times 10^{-5} & -0.009095 \\ -0.100859 & 0.798642 & -0.001513 & 0.030154 & -0.088679 \\ 2.788025 & 0.022924 & 0.041603 & 0.024368 & -0.465253 \end{bmatrix},$$

$$B_c = \begin{bmatrix} -0.000617 & -0.017424 & -2.871137 \\ 0.792006 & -1.103803 & 1.684791 \\ -0.99029 & -0.770164 & 12.026577 \\ -0.582481 & 0.746858 & -0.299745 \\ 0.011564 & 0.039367 & 11.985945 \end{bmatrix}, \quad C_c = \begin{bmatrix} 0.006534 & 0.005311 \\ 0.000239 & -0.001499 \\ -0.002763 & -0.002579 \\ 0.000115 & -9.579 \times 10^{-5} \\ -0.000843 & -0.001116 \end{bmatrix}^\top,$$

$$D_c = \begin{bmatrix} -0.002889 & -0.001835 & -5.217 \times 10^{-6} \\ -0.001533 & -0.003218 & -4.493 \times 10^{-6} \end{bmatrix}.$$

In addition, $\gamma = 0.866$, which gives a guaranteed radius of stability margins $r_1 = r_2 = r^0/\gamma = 0.808$ at the plant's inputs and is very significant from the engineering point of view. The factual values of r_1 and r_2 will be determined below.

The eigenvalues of the closed-loop system matrix A_{cl} satisfy the inequality

$$\max |\lambda_i(A_{cl})| = 0.8019 < 1/\alpha.$$

Hence, the settling time requirements hold.

Figure 4 presents the simulation results for the closed-loop system under the step external disturbance $f = 600$ Nm. On the left, the solid line corresponds to transients for y_1 and the dashed line to those for y_2; on the right, the solid line corresponds to transients for y_3. According to the transient plots, the accuracy requirements are true for all controlled variables, and the equal-load requirement of the drives holds for y_1 and y_2. The same figure demonstrates that the factual settling time matches the desired one $t_p = 0.25$ s.

Figure 5 shows the amplitude-frequency response of the transfer function $|T_{y_3 f}|$ of the closed-loop system relating the external disturbance to the main controlled variable, scaled by a disturbance amplitude of 600. Its maximum falls at the frequency $\omega = 7.14$ rad/s, being equal to 0.945 rad/s. The absolute value of the frequency response for the step disturbance (at $\omega = 0$) is 0.944 rad/s. In other words, the error under the worst-case disturbance slightly differs from the error under the step disturbance, as stated above.

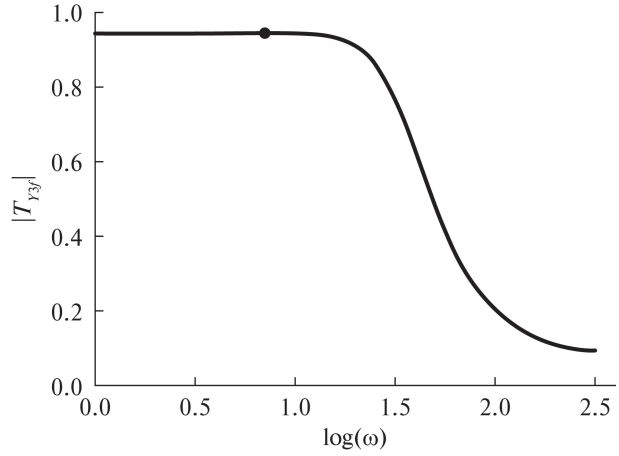

Fig. 5. The absolute value of the amplitude-frequency response $|T_{y_3 f}|$.

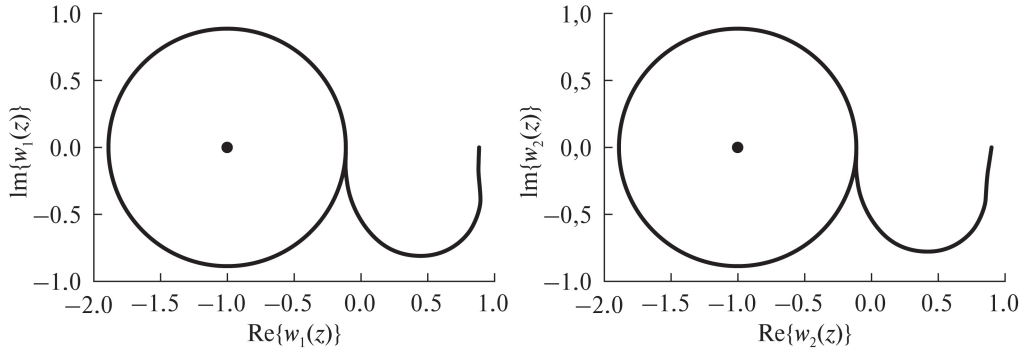

Fig. 6. The radii of stability margins and Nyquist plots (break points at inputs): w_1(z) (left) and w_2(z) (right).

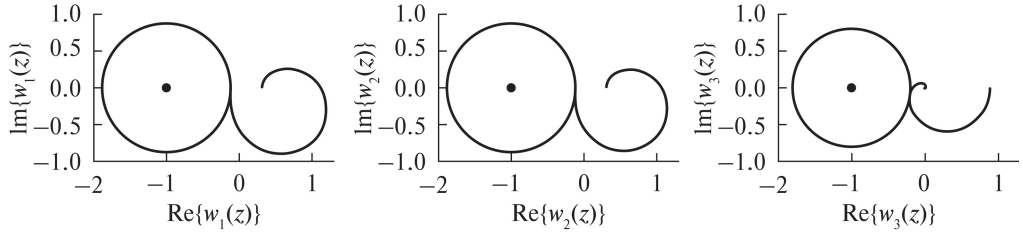

Fig. 7. The radii of stability margins and Nyquist plots (break points at outputs).

Note that the steady-state error for the main controlled variable turned out to be very close to the given one, indicating a low degree of sufficiency of the design procedure by this performance index.

The factual robust properties of the closed-loop system at the input and output are determined using the Nyquist plots of the open-loop system drawn by breaking at the corresponding points.

Figure 6 provides the Nyquist plots of the open-loop system when the break points are at the inputs u_1 (on the left) and u_2 (on the right). Also, see the critical points $(-1,\ j0)$ in this figure, around which circles with radii $r_1 = 0.881$ (on the left) and $r_2 = 0.889$ (on the right) are drawn. These circles determine the factual radii of stability margins at the plant's input.

Next, Fig. 7 shows the Nyquist plots of the system when the break points are at the outputs: from left to right, the cases of y_1, y_2, and y_3, respectively. As for the inputs, the radii of the circles in Fig. 7 are equal to the corresponding factual radii of stability margins at the outputs: $r_1 = 0.882$, $r_2 = 0.887$, and $r_3 = 0.803$.

Note that the controller designed ensures high stability margins at all inputs and outputs.

Of particular attention is the stability of the systems broken at separate inputs and outputs of the plant. This is quite important under the possible saturation of the corresponding signals and their shelving.

Finally, we emphasize that the discrete-time controller ensures significantly higher radii of stability margins for all control and measured variables (except for the main one, angular velocity) than the continuous controllers for this plant [21, 31, 33]. In particular, the radius of stability margins was about 0.45 at all outputs (where it was ensured) and inputs and 0.99 for the main controlled variable.

6. CONCLUSIONS

This paper has proposed an approach to designing discrete-time output-feedback controllers for multivariable systems that ensure desired or achievable control performance indices: errors for each controlled variable, settling time, and the radii of stability margins at the plant's input.

The class of external disturbances considered above is rather wide and covers elementwise bounded functions: $\forall k\ |w_i(k)| \leqslant w_i^*,\ i = \overline{1,m}$. Note that the continuous prototype of such disturbances is continuous and piecewise differentiable functions of time; therefore, they can be represented by an absolutely convergent Fourier series [21]. Only such disturbances are encountered in engineering practice.

We list several advantages of the design method over the known ones:

1. The original problem is solved via the standard discrete H_∞ optimization procedure with analytical formulas for assigning the weights of the objective functional for a given accuracy.

2. There is a very important, from the engineering point of view, physical interpretation of the frequency matrix inequality for the transfer matrix of the open-loop system in the language of Nyquist plots of the system broken at the ith input of the plant. (In contrast to [21], this inequality ensures individual radii of stability margins.)

3. The absolute stability of the closed-loop system with sector nonlinearities at possibly all physical inputs of the plant has been proved. For each input, the size of the nonlinearity sector is uniquely determined by the radii of stability margins ensured by the controller designed. This feature is also crucial from the engineering point of view.

4. The controller's order does not exceed that of the plant, which is very valuable in applications.

5. The degree of sufficiency of this method is significantly lower compared to those proposed previously [21, 31] owing to a two-fold reduction in the number of block elements in the transfer matrix of the closed-loop system (13), which is subjected to the H_∞ optimization procedure.

The latter is made possible by applying an external disturbance consistently with a control action. This condition can be considered to be valid for the vast majority of electromechanical systems: physically a control action from a digital controller is applied to a plant indirectly, through an actuator representing a power amplifier with a gain much greater than unity. This explains the significantly greater influence of a disturbance applied consistently with a control action on controlled variables compared to that applied as a load moment. The controller design approach proposed above has been illustrated by a numerical example arising in engineering practice (a pipe-electric welding machine operating at the Elektrostal Heavy Engineering Works).

APPENDIX

Proof of Lemma 1. As $k \to \infty$, the forced oscillations at the output of system (1), (2) are described by

$$y_i(k) = \sum_{j=1}^{\infty} a_i(\omega_j) \sin(\omega_j kh + \phi_i(\omega_j)), \quad i = \overline{1, m_2}, \tag{A.1}$$

where $a_i(\omega_j) \geqslant 0$ and $\phi_i(\omega_j)$ are the amplitudes and phases of the oscillations at the plant's output caused by the jth harmonic in the input signal (3).

The signal (A.1) describes the steady-state process at the plant's output. At the time instant $t_p = k_p h$, it differs from the factual value of the plant's output by at most 5% due to the discrete function $e_i(k)$, which vanishes at the rate of a geometric progression. Therefore, the plant's output $y_i(k)$ will be considered below without these components.

In each coordinate of the vector y, the amplitudes of oscillations with the frequency ω_j in (A.1) are the absolute values of the corresponding components of the complex conjugate vectors $T_{yw}(e^{j\omega_j h})w_+^{(j)}$ and $T_{yw}(e^{-j\omega_j h})w_-^{(j)}$, where

$$w_+^{(j)} = [w_{1j}e^{j\phi_{1j}},\ w_{2j}e^{j\phi_{2j}},\ \ldots,\ w_{mj}e^{j\phi_{mj}}]^\top,$$
$$w_-^{(j)} = [w_{1j}e^{-j\phi_{1j}},\ w_{2j}e^{-j\phi_{2j}},\ \ldots,\ w_{mj}e^{-j\phi_{mj}}]^\top.$$

Indeed, the jth harmonic of the input vector w can be written as $(w_+^{(j)}e^{j\omega_j kh} - w_-^{(j)}e^{-j\omega_j kh})/(2j)$.

We find a partial solution $x_{cl}(k)$ of the equations of the closed-loop system (1), (2) with $w(k) = w_+^{(j)}e^{j\omega_j kh}$. Let the closed-loop system equations be denoted by

$$\begin{aligned} x_{cl}(k+1) &= A_{cl}x_{cl}(k) + B_{cl}w(k), \\ y(k) &= C_{cl}x_{cl}(k), \quad k = 1, 2, \ldots, \end{aligned} \tag{A.2}$$

where the matrix A_{cl} has been described above, $B_{cl} = [B^\top,\ 0^\top]^\top$, and $C_{cl} = [C,\ 0]$. Substituting $w(k) = w_+^{(j)}e^{j\omega_j kh}$ into the first formula of (A.2) yields

$$x_{cl}(k+1) = A_{cl}x_{cl}(k) + B_{cl}w_+^{(j)}e^{j\omega_j kh}.$$

The partial solution of the system is represented as $x_{cl}(k) = x^{(j)}e^{j\omega_j kh}$, where $x^{(j)} \in \mathbb{C}^{n+n_c}$ is the vector of complex numbers; then $x_{cl}(k+1) = x^{(j)}e^{j\omega_j (k+1)h} = x^{(j)}e^{j\omega_j h}e^{j\omega_j kh}$. We substitute this expression into (A.2) to obtain

$$x^{(j)}e^{j\omega_j h}e^{j\omega_j kh} = A_{cl}x^{(j)}e^{j\omega_j kh} + B_{cl}w_+^{(j)}e^{j\omega_j kh}$$

and, after some simplifications,

$$x^{(j)} = \left(e^{j\omega_j kh}I - A_{cl}\right)^{-1} B_{cl}w_+^{(j)}.$$

Then $x_{cl}(k) = \left(e^{j\omega_j kh}I - A_{cl}\right)^{-1} B_{cl}w_+^{(j)}e^{j\omega_j kh}$ and, considering $y(k) = C_{cl}x_{cl}(k)$, it follows that

$$y_+(k) = T_{yw}(e^{j\omega_j h})w(k),$$

where $T_{yw}(e^{j\omega_j h}) = C_{cl}\left(e^{j\omega_j kh}I - A_{cl}\right)^{-1} B_{cl}$ is the transfer matrix relating w to y. By analogy, for $w(k) = w_-^{(j)}e^{-j\omega_j kh}$, we arrive at $y_-(k) = T_{yw}(e^{-j\omega_j h})w_-^{(j)}e^{-j\omega_j kh}$.

According to the superposition principle, for the jth harmonic of the output vector y with the components from (A.1), it is easy to derive

$$(y_+ - y_-)/(2j) = \left[T_{yw}(e^{j\omega_j h})w_+^{(j)}e^{j\omega_j kh} - T_{yw}(e^{-j\omega_j h})w_-^{(j)}e^{-j\omega_j kh}\right]/(2j).$$

Obviously, $a_i^2(\omega_j) = y_{i-}y_{i+}$, where y_{i-} and y_{i+} are the ith components of the vectors y_- and y_+, respectively. Then, in view of the diagonal structure of the matrix Q, we write

$$\sum_{i=1}^{m_2} q_i a_i^2(\omega_j) = y_-^\top Q y_+ = {w_-^{(j)}}^\top T_{yw}^\top(e^{-j\omega_j h})QT_{yw}(e^{j\omega_j h})w_+^{(j)}.$$

Considering the right-hand side of inequality (16), it follows that

$$\sum_{i=1}^{m_2} q_i a_i^2(\omega_j) \leqslant \gamma^2 {w_-^{(j)}}^\top w_+^{(j)} = \gamma^2 \sum_{p=1}^{m} w_{pj}^2$$

and, consequently, $q_i a_i^2(\omega_j) \leqslant \gamma^2 {w_-^{(j)}}^\top w_+^{(j)} = \gamma^2 \sum\limits_{p=1}^{m} w_{pj}^2,\ i = \overline{1, m_2}$.

Extracting the square roots of both sides of the last inequality yields

$$\sqrt{q_i}a_i(\omega_j) \leqslant \gamma\sqrt{\sum_{p=1}^{m} w_{pj}^2} \leqslant \gamma\sqrt{\left(\sum_{p=1}^{m} w_{pj}\right)^2}, \quad i = \overline{1, m_2};$$

therefore, $\sqrt{q_i}a_i(\omega_j) \leqslant \gamma \sum\limits_{p=1}^{m} w_{pj},\ i = \overline{1, m_2}$. Summing over all frequencies, we obtain

$$\sqrt{q_i}\sum_{j=1}^{\infty} a_i(\omega_j) \leqslant \gamma \sum_{p=1}^{m}\sum_{j=1}^{\infty} w_{pj}, \quad i = \overline{1, m_2}.$$

Due to $y_{i,st} \leqslant \sum\limits_{j=1}^{\infty} a_i(\omega_j),\ i = \overline{1, m_2}$, and (4), we finally get

$$\sqrt{q_i}y_{i,st} \leqslant \gamma \sum_{p=1}^{m}\sum_{j=1}^{\infty} w_{pj} \leqslant \gamma \sum_{p=1}^{m} w_p^*, \quad i = \overline{1, m_2},$$

which implies (17).

REFERENCES

1. Voronov, A.A., *Osnovy avtomaticheskogo upravleniya. Avtomaticheskoe regulirovanie neprerыvnykh lineinykh sistem* (Foundations of Automatic Control Theory. Automatic Regulation of Continuous Linear Systems), Moscow: Energiya, 1980.
2. MacFarlane, A.G.J., The Development of Frequency-Response Methods in Automatic Control, *IEEE Trans. Autom. Control*, 1979, vol. 24, no. 2, pp. 250–265.
3. Solodovnikov, V.V., *Osnovy avtomaticheskogo regulirovaniya* (Foundations of Automatic Regulation), Moscow: Mashgiz, 1954.
4. Solodovnikov, V.V., *Automatic Control & Computer Engineering*, vol. 1, Pergamon Press, 1961; vol. 2, Pergamon Press, 1963.

5. Besekerskii, V.A. and Fabrikant, E.A., *Dinamicheskii sintez sistem giroskopicheskoi stabilizatsii* (Dynamic Design of Gyro Stabilization Systems), Leningrad: Sudostroenie, 1968.

6. Besekerskii, V.A. and Popov, E.P., *Teoriya sistem avtomaticheskogo regulirovaniya* (Theory of Automatic Regulation Systems), Moscow: Nauka, 1975.

7. Barabanov, A.E., *Sintez minimaksnykh regulyatorov* (Minimax Controller Design), St. Petersburg: St. Petersburg State University, 1996.

8. Dahleh, M. and Diaz-Bobillo, I.J., *Control of Uncertain Systems: A Linear Programming Approach*, New Jersey: Prentice Hall, 1995.

9. Zhou, K., Doyle, J., and Glover, K., *Robust and Optimal Control*, New Jersey: Prentice Hall, 1996.

10. Zhou, K. and Doyle, J., *Essentials of Robust Control*, New Jersey: Prentice Hall, 1998.

11. Skogestad, S. and Postlethwaite, I., *Multivariable Feedback Control: Analysis and Design*, New Jersey: John Wiley & Sons, 2006.

12. Chestnov, V.N., Fundamental Features of Discrete-Time Control Systems and Reachable Values of Engineering Performance Indices, *Trudy 14-go Vserossiiskogo soveshchaniya po problemam upravleniya* (Proceedings of the 14th All-Russian Meeting on Control Problems), Moscow, 2024, pp. 75–79.

13. Polyak, B.T., Khlebnikov, M.V., and Shcherbakov, P.S., *Upravlenie lineinymi sistemami pri vneshnikh vozmushcheniyakh: tekhnika lineinykh matrichnykh neravenstv* (Control of Linear Systems under Exogenous Disturbances: The Technique of Linear Matrix Inequalities), Moscow: LENAND, 2014.

14. Aleksandrov, A.G., Roughness Criteria for Time-Varying Automatic Control Systems, in *Analiticheskie metody sinteza regulyatorov* (Analytic Controller Design Methods), Saratov: Saratov Polytechnic Institute, 1980, pp. 3–14.

15. Chestnov, V.N., Synthesis of Controllers for Multivariable Systems with a Given Radius of Stability Margin by the H_∞-optimization Method, *Autom. Remote Control*, 1999, vol. 60, no. 7, pp. 986–993.

16. Aström, K.J. and Murray, R.M., *Feedback Systems: an Introduction for Scientists and Engineers*, New Jersey: Princeton University Press, 2008.

17. Chestnov, V.N., Synthesis of Discrete H_∞-Controllers with Given Stability Margin Radius and Settling Time, *Autom. Remote Control*, 2014, vol. 75, no. 9, pp. 1593–1607.

18. Chestnov, V.N., Maximum Achievable Precision of Linear Systems with Discrete Controllers, *Autom. Remote Control*, 2014, vol. 75, no. 2, pp. 333–350.

19. Chestnov, V.N., Design of Robust H_∞-controllers of Multivariable Systems Based on the Given Stability Degree, *Autom. Remote Control*, 2007, vol. 68, no. 3, pp. 557–563.

20. Chestnov, V.N. and Shatov, D.V., Design of Given Oscillation Index Scalar Controllers: Modal and H^∞-Approaches, *Autom. Remote Control*, 2020, vol. 81, no. 3, pp. 517–527.

21. Chestnov, V.N., Synthesis of Multivariable Systems According to Engineering Quality Criteria Based on H_∞-Optimization, *Autom. Remote Control*, 2019, vol. 80, no. 10, pp. 1861–1877.

22. Chestnov, V.N. and Shatov, D.V., Design of H_∞ Discrete-Time Controllers for Multivariable Systems via Given Engineering Performance Indices, *Proc. of 23rd International Conference on System Theory, Control and Computing (ICSTCC 2019)*, 2019, pp. 424–429.

23. Chestnov, V.N. and Shatov, D.V., Discrete-Time Controller Design for Multivariable Systems by Engineering Performance Criteria, *Trudy 14-go Vserossiiskogo soveshchaniya po problemam upravleniya* (Proceedings of the 14th All-Russian Meeting on Control Problems), Moscow, 2024, pp. 418–422.

24. Chestnov, V.N., Synthesizing H_∞-Controllers for Multidimensional Systems with Given Accuracy and Degree of Stability, *Autom. Remote Control*, 2011, vol. 72, no. 10, pp. 2161–2175.

25. Anderson, B.D.O. and Moore, J.B., *Optimal Control: Linear Quadratic Methods*, New Jersey: Prentice Hall, 1989.

26. *The Control Handbook*, Levine, W.S., Ed., IEEE Press, 1996.

27. Chestnov, V.N. and Shatov, D.V., Robust Controller Design for Multivariable Systems under Non-stationary Parametric Variations and Bounded External Disturbances, *Autom. Remote Control*, 2024, vol. 85, no. 6, pp. 562–575.

28. Tsypkin, Ya.Z., *Osnovy teorii avtomaticheskikh sistem* (Foundations of the Theory of Automatic Systems), Moscow: Nauka, 1977.

29. Yakubovich, V.A., Absolute Stability of Pulse Systems with Several Nonlinear or Linear Non-Stationary Blocks. I, *Autom. Remote Control*, 1967, vol. 28, no. 9, pp. 1301–1313.

30. Yakubovich, V.A., Absolute Stability of Pulse Systems with Several Nonlinear or Linear Non-Stationary Blocks. II, *Autom. Remote Control*, 1968, vol. 29, no. 2, pp. 244–263.

31. Chestnov, V.N. and Shatov, D.V., Multivariable Systems Design of Desired Accuracy Based on *LQ* and H_∞ Optimization Procedures, *Proc. of the 2018 European Control Conference (ECC-2018)*, 2018, pp. 2511–2516.

32. Åström, K.J. and Hagglund, T., *Advanced PID Control*, NC: ISA, 2006.

33. Chestnov, V.N. and Shatov, D.V., Design of Multivariable Tracking Systems via Engineering Performance Indices Based on H_∞ Approach, *Control Sciences*, 2021, no. 3, pp. 29–36. http://doi.org/10.25728/cs.2021.3.4

This paper was recommended for publication by A.I. Matasov, a member of the Editorial Board